Impulse Generation by an Open Shock Tube

J. Kasahara*
University of Tsukuba, Tsukuba 305-8573, Japan
Z. Liang†, S.T. Browne‡, and J.E. Shepherd§
Aeronautics, California Institute of Technology, Pasadena, CA 91125

Submitted August 23, 2006

Abstract

We performed experimental and numerical studies of a shock tube with an open end. The purpose was to investigate the impulse due to the exhaust of gases through the open end of the tube as a model for a partially-filled detonation tube as used in pulse detonation engine testing. We have studied the effects of the pressure ratio (varied between 3 to 9.4) and volume ratio (expressed as fill fraction) between the driver and driven section. Two different driver gases, helium and nitrogen, and fill fractions between 5 and 100% were studied; the driven section was filled with air. For both driver gases, increasing the pressure ratio led to larger specific impulses. The specific impulse increased for decreasing fill fraction for the helium driver but the impulse was almost independent of fill fraction for the nitrogen driver. Two-dimensional (axi-symmetric) numerical simulations were carried out for both driver gases. The simulation results show reasonable agreement with experimental measurements at high pressure ratios or small fill fractions but there are substantial discrepancies for the smallest pressure ratios studied. Empirical models for the impulse in the limits of large and small fill fractions are also compared to the data. Reasonable agreement is found for the trends with fill fraction using the Gurney or Sato et al. model and the bubble model of Cooper is able to predict the small fill fraction limit in both cases.

---

*Assistant Professor

†Postdoctoral Scholar

‡Graduate Student

§Professor

Introduction

Motivated by recent interest in pulse detonation engines,[1] the impulse from a partially-filled detonation tube has been studied by a number of researchers.[2–11] In these experiments and analysis, a portion of the detonation tube near the closed end (thrust surface) contains the combustible mixture while the remaining portion of the tube up to the open end contains an inert gas mixture, .e.g., air. The general conclusions of these studies is that an inert section will increase the specific impulse (impulse per unit mass of combustible mixture) although the total impulse decreases. Based on these studies, the use of partially-filled detonation tubes has been proposed as a technique for improving specific performance. A number of simple models have been proposed to account for the partial-fill effect but there is no consensus regarding the best way to model this effect and correlate performance. It is hard to make detailed comparisons between experiments and models because it is difficult to generate an ideal detonation in a small length tube, and non-ideal processes such as heat transfer losses may be significant.[12,13]

For these reasons, we are motivated to examine the simpler case of a shock tube with an open end. Experimentally, we can more readily vary parameters including the fill fraction and the initial pressure ratio than is possible in detonation experiments. Numerically, the non-reacting gas dynamics of the shock tube can be accurately simulated using the perfect gas models for the driver and driven section. We can examine the limiting value of impulse as the fill fraction approaches zero and compare the results with models proposed for this case. Cooper[6] predicted that the impulse will approach a limiting value on the basis of a simple model, but it is experimentally difficult to approach this limit in the detonation case. Other approximate models[5,8,11,12] have also been proposed to predict impulse dependence on the fill fraction when the fill fraction is close to one. We have examined both limits experimentally, carried out detailed numerical simulations, and compared the results to the approximate analytical models.

Experiments

As shown in Figure 1, the experimental apparatus was a partially-filled shock tube. This conventional shock tube consisted of a cylindrical driver of fixed length (100.7 mm) to which cylindrical extensions (the driven section) of various lengths (12.7-1814 mm) were added. The driver section was filled with pressurized gas (helium or nitrogen) and initially sealed by a thin polyethylene-terephthalate plastic diaphragm separating the driver and driven section. The driven section was open to the atmosphere. The initial conditions in the driven section matched those of the room, nominally 22°C and $P_a = 99$ kPa. In the driver section, the initial temperature was also room temperature , but the initial pressure was varied from P_0

= 929 kPa ($P_0/P_a = 9.38$) to $P_0 = 198$ kPa ($P_0/P_a = 2.0$).

To start the experiment, the diaphragm was ruptured using a pneumatically-activated cutter. The pressurized driver gas expanded into the driven section, creating a shock in the driven section which propagated to the open end of the driven section and diffracted into the surrounding atmosphere. This resulting wave system is similar to that observed in detonation tube experiments and models.[12,14] An expansion wave (E_1), centered at the initial location of the diaphragm, propagated toward the thrust surface, the closed end wall of the driver section. This process is illustrated in Fig. 2. Initially, the pressure on the closed end surface was equal to the initial pressure of the driver, P_0 and remained constant in the interval t_0-t_1. During the initial reflection of the expansion wave the pressure decreased during the time interval t_1-t_2 and remained constant again during the interval t_2-t_3. After sufficient time for reverberation, the pressure inside the tube reached the ambient value P_a. As shown in Figure 3, the impulse was measured mechanically using the ballistic pendulum technique[15] and the pressure history on the closed end was measured with a piezoelectric pressure transducer (PCB 113A). The partially-filled shock tube was suspended by four stainless wires from the ceiling of the experimental room. The effective wire length of the pendulum L was 1987 mm. The maximum displacement of the shock tube in the horizontal direction x_m was measured by using CCD camera. When $L >> x_m$, the impulse I was easily obtained by Eqn. 1

$$I = M x_m \sqrt{\frac{g}{L}}, \tag{1}$$

where M is the mass of the partially-filled shock tube, and g is gravitational acceleration. The specific impulse was obtained by Eqn. 2

$$I_{sp} = \frac{I}{m_0 g} = \frac{M x_m}{\rho_0 V_0} \sqrt{\frac{1}{gL}}, \tag{2}$$

where m_0, ρ_0 and V_0 are the mass, initial density, and initial volume of the driver gas (helium or nitrogen) respectively.

Numerical Model

The computational domain is shown in Fig. 4. Since the geometry is symmetric, only half of the domain was computed. The tube diameter, $d = 39.5$ mm, and driver section length, $L_0 = 101.6$ mm, are constant. The driven section varies between 0 m and 1.8339 m. The fill fraction, α, is defined as $\alpha = L_0/L$, where L is the total shock tube length. The total computational domain size is $3L$ (length) by $4d$ (width). An outflow boundary condition is implemented on the top, left (except the the closed end of the shock tube), and right sides.

The bottom side is the symmetry boundary. The corresponding gas parameters are listed in Table 1.

The problem is modeled using the two-dimensional (planar), inviscid, non-reactive Euler equations with the perfect gas equation of state. Two constant polytropic exponents, γ_1 and γ_2, representing gases in both driver and driven sections are used. Each gaseous species is assumed to be a thermally perfect gas, so the specific heat at constant pressure

$$c_{p_i} = c_{p_i}(T) \tag{3}$$

is function of temperature only, where $i = 1, 2$. For a perfect gas,

$$c_{p_i} = \frac{\gamma_i R}{\gamma_i - 1}. \tag{4}$$

The specific heat for the mixture is then given by

$$c_p(Y_i, T) = \sum_{i=1,2} Y_i c_{p_i}(T) \tag{5}$$

where Y_i is the mass fraction of gases. The details of the implementation of the mixture model are given in Deiterding.[16]

The equations are solved with an explicit second order Godunov-type numerical scheme incorporating a hybrid Roe-solver-based method. A block-structured adaptive mesh refinement technique is utilized to supply the required resolution locally.[17] This adaptive method uses a hierarchy of spatially-refined subgrids which are integrated recursively with reduced time steps.

In the numerical simulations, the impulse was computed by first finding the spatial average of the pressure on the closed end to determine the net force on the tube as a function of time. The force was then numerically integrated in time to find the total impulse.

$$I = \int F dt = \int_0^{t_{final}} (P(t) - P_a) A_0 dt \tag{6}$$

where $P(t)$ is the average pressure on the thrust surface, P_a is the ambient pressure, A_0 is the cross-sectional area of the driver section, and t_{final} is the final time reached in the simulation. The simulation was carried out until $P(t)$ was reasonably close to P_a. The trapezoidal rule was used to perform the integration and in the current computations, t_{final} = 4 ms for helium and t_{final} = 8 ms for nitrogen.

The specific impulse based on the total driver mixture mass is defined as

$$I_{sp} = \frac{I}{\rho_0 V_0 g} = \int_0^{t_{final}} \frac{(P(t) - P_a)}{\rho_0 L_0 g} dt \tag{7}$$

where ρ_0 and L_0 are the gas density and the tube length of the driver section respectively.

Approximate Models

A number of approximate models have been proposed for correlating impulse with the fill fraction and the thermodynamic properties of the mixture. We have examined three of these in the present study: the Gurney model, based on energy conservation, a "bubble" model based on acoustic analysis, and an empirical model by Sato et al.[11] The Gurney and Sato models are useful for large fill fractions while the "bubble" model is designed to deal with the limiting case of a very small fill fraction.

Gurney model

The Gurney model was originally developed to predict the acceleration of metal by detonation of explosives.[18,19] The model is based on energy conservation and a simple approximation of the velocity in the detonation products. The Gurney model for explosives suggests a simple approach for predicting the value of the impulse for pulse detonation tubes[5,6] and can be extended to the present case by analogy. The results of the Gurney model can be expressed in terms of the mass M of the shock tube, mass C of the pressurized driver gas, and mass N of the air in the driven section, which is referred to as the "tamping" mass in the case of explosives. The impulse predicted[5] by the Gurney model is

$$I = M\sqrt{2e}\left(\sqrt{\frac{1+A^3}{3(1+A)} + A^2\frac{N}{C} + \frac{M}{C}}\right)^{-1} \tag{8}$$

where

$$A = \frac{1+2\frac{M}{C}}{1+2\frac{N}{C}} \tag{9}$$

and e is the Gurney energy of the explosive, in this case, the pressurized driver gas. The Gurney energy is taken to be a percentage of the ideal amount of specific energy available to do mechanical work

$$e = \eta e_i \tag{10}$$

η is the energy efficiency and is determined empirically (see Section). Assuming isentropic expansion of the pressurized gas,

$$e_i = \frac{P_0}{(\gamma-1)\rho_0}\left[1-\left(\frac{P_0}{P_a}\right)^{1/\gamma-1}\right] \tag{11}$$

Typically, $M/C \to \infty$, and we can rewrite Eq. 8 in term of the specific impulse

$$I_{sp}(\alpha) = \frac{I}{Cg} = \frac{\sqrt{2e}}{g}\frac{\frac{N}{C}+\frac{1}{2}}{\sqrt{\frac{N}{C}+\frac{1}{3}}} \tag{12}$$

The mass of the pressurized gas C and the mass of the air N can be related to the partial fill fraction α

$$\alpha = \frac{\frac{C}{\rho_0}}{\frac{C}{\rho_0}+\frac{N}{\rho_a}} = \frac{1}{1+\frac{\rho_0}{\rho_a}\frac{N}{C}} \tag{13}$$

where ρ_a is the density of the air. Therefore for a given gas in the driver section, the specific impulse depends on the fill fraction α and the Gurney energy e.

For a fully-filled tube, i.e. without any tamping gas ($N = 0$), $\alpha = 1.0$, and the specific impulse $I_{sp}(\alpha = 1)$ is

$$I_{sp}(\alpha = 1) = \frac{\sqrt{1.5e}}{g} \tag{14}$$

Then the ratio of $I_{sp}/I_{sp}(\alpha = 1)$ is

$$\frac{I_{sp}}{I_{sp}(\alpha = 1)} = \sqrt{\frac{4}{3}}\frac{\frac{N}{C}+\frac{1}{2}}{\sqrt{\frac{N}{C}+\frac{1}{3}}}, \tag{15}$$

which only depends on the ratio of N/C or the fill fraction α.

Table 2 shows the specific impulse $I_{sp}(\alpha = 1)$ computed with Eq. 12. For explosives, the Gurney energy is some fraction of the heat of combustion of the explosive and we expect in the present case that it will be some fixed fraction η of the ideal energy given by Eq. 11. For detonation tubes, a value of $\eta = 0.3$ was determined.[5,6] For the present case, we have determined the efficiency in Section by fitting the Gurney model results to either the experimental data or computation results.

Bubble model

The expanding "bubble" model of detonation hot products[6] predicts the specific impulse in the limit of $\alpha \to 0$. Here we use the same idea to analyze the shock tube. If the pressurized driver gas expands isentropically and is spatially uniform, the change in pressure, $P(t)$, can

be related to the length of the driver as a function of time

$$P(t) = P_0 \left(\frac{L_0}{x(t)} \right)^{\gamma_0} \tag{16}$$

where $x(t)$ is the location of the contact surface that separates the driver and driven gas in an ideal one-dimensional shock tube model. The idea behind the bubble model is that the contact surface velocity induces a flow and pressure rise in the driver gas which, for small velocities, can be computed using the method of characteristics or in a linearized version, acoustic theory. This yields[6] an ordinary differential equation for contact surface velocity

$$\frac{dx}{dt} = \frac{2c_0}{\gamma_a - 1} \left(\frac{x}{L_0} \right)^{\frac{\gamma_0}{2\gamma_a}(1-\gamma_a)} \left(\frac{P_0}{P_a} \right)^{\frac{1}{2\gamma_a}(\gamma_a - 1)-1} \tag{17}$$

where γ_0 and γ_a represent the specific heat ratio of the driver gas and the air. Equation 17 can be numerically integrated until the contact surface reaches the final position. Time integration of the pressure history at the closed end yields the predicted impulse. Figure 5a shows an x-t diagram of the contact surface trajectories for several cases. The pressure histories for several pressure ratios are plotted in Fig. 5b. The pressure decays faster for higher initial pressure ratios and larger specific heat ratios, γ, in the driver gas.

Table 3 lists the specific impulse in the limit of $\alpha \to 0$ or $L \to \infty$, $I_{sp}(\alpha \to 0)$, computed with Eq. 17 for each case.

Sato model

Sato et al.[11] proposed a simple empirical formula for predicting $I_{sp}/I_{sp}(\alpha = 1)$,

$$I_{sp}/I_{sp}(\alpha = 1) = \frac{1}{\sqrt{Z}} \tag{18}$$

where Z is related to the fill fraction α by

$$Z = \frac{\alpha \rho_0}{\alpha \rho_0 + (1 - \alpha)\rho_a}, \tag{19}$$

Z can also be related to the mass ratio of N/C by substituting Eq. 13 to Eq. 19,

$$Z = \frac{1}{1 + N/C}. \tag{20}$$

Now Eq. 18 becomes

$$\frac{I_{sp}}{I_{sp}(\alpha = 1)} = \sqrt{1 + \frac{N}{C}} \tag{21}$$

Comparison with the Gurney model and simulation results will be discussed in the following Section.

Simulation and Experimental Results

Pressure and impulse history

Figure 6 shows simulation results of the average pressure time histories on the thrust surface and the specific impulse for two fill fractions with helium as the driver gas. Since the length of the driver is fixed, the time, t_1 (Fig. 2), when the head of the expansion fan (E_1) radiating from the location of the diaphragm reaches the thrust surface only varies with driver gas. This is because the speed of the expansion fan is determined by the sound speed in the driver gas. The sound speed in helium is 1008 m/s, so t_1 is ≈ 0.1 ms. For the maximum fill fraction, $\alpha = 1.0$ (Figure 6a), the pressure on the thrust surface, $P(t)$, decays below the ambient pressure P_a between $0.1 - 0.12$ ms depending on the pressure ratio. Then it begins to oscillate, but all oscillations are damped out by 4 ms for all pressure ratios. In each case, the specific impulse reaches its maximum value when $P(t) = P_a$ and then decreases to its minimum value due to the negative impulse generated when $P(t) < P_a$. The final average I_{sp} is close to the maximum I_{sp} for higher pressure ratios, but in the case $P_0/P_a = 3$, it is almost 30% lower than its maximum. The same feature in the pressure signals was observed in the experiments, shown in Fig. 7. In the experiments, the time zero corresponds to when the data acquisition system was triggered and the negative time period represents the pre-trigger signals.

In the computations, before $P(t)$ decays below P_a in the lower fill fraction case, $\alpha = 0.6$ (Figure 6b), there exists a second plateau. In this case, the expansion wave (E_3), which is radiating toward the thrust surface from the interaction of the reflected expansion fan (E_2) and the contact surface, must travel farther as the length of the driven section is longer. In the lower fill fraction case, E_3 reaches the thrust surface later than in the $\alpha = 1.0$ case. Hence the total impulse is larger than the $\alpha = 1.0$ case at the same pressure ratio. The pressure oscillations are also damped more quickly than in the $\alpha = 1.0$ case.

The pressure and specific impulse histories for nitrogen are shown in Fig. 8. Since the sound speed in nitrogen (350 m/s) is lower than in helium, t_1 occurs relatively later, 0.29 ms. The second-constant-pressure stage does not appear for all fill fractions and pressure ratios, because the pressure oscillates for a much longer time period ($t_{final} > 8$ ms). The oscillation period is shorter for larger fill fraction, i.e. $t_{final} = 1.8$ ms for $\alpha = 0.8$ and $t_{final} = 3$ ms for $\alpha = 0.2$. The fill fraction has a stronger effect on the final average specific impulse than does the initial pressure ratio. For example, when $\alpha = 1.0$, the final average I_{sp} is slightly below its maximum value for all three pressure ratios, but for $\alpha = 0.2$, it varies widely ($8 - 22$ s

for $P_0/P_a = 3$) mainly due to the long oscillation period. For this reason, longer integration time periods are necessary for nitrogen mixtures at low fill fractions.

Specific impulse

The specific impulse computed from numerical simulations, analytical models, and experimental measurements are compared in Figures 9-12.

Effect of fill fraction

For helium, the general trend is that the I_{sp} increases as α decreases until $\alpha < 0.2$ where the I_{sp} reaches a maximum value. For nitrogen, the I_{sp} remains almost constant as α varies. For both gases, the I_{sp} increases as the pressure ratio increases for a fixed α. In Figures 9-11 and 12, two Gurney model estimates are computed with different energy efficiencies.

For $P_0/P_a = 9.38$ (Fig. 9) and $P_0/P_a = 6.0$ (Fig. 10), when $\alpha < 0.2$, results from the bubble model show close agreement with experiments and simulations for helium, but slightly underpredict for nitrogen. When $0.2 < \alpha < 0.8$, solutions from the Gurney model also match well with both experiments and simulations. When $\alpha > 0.8$, simulation results are systematically higher than experimental data (25%). For $P_0/P_a = 3.0$ (Fig. 11), simulation results are quite different from the experiments when $0.4 < \alpha < 0.8$. We believe that this is due to two factors. First, in the experiment, the method with which the diaphragm was broken may have caused finite delay time of its rupture which affects the measurements. Experimental pressure profiles at the thrust wall for different initial pressure ratios are shown in Fig. 7. For a low pressure ratio, $p1/pa = 3.134$, the decay time at the wall becomes longer than in Fig. 6a. When the pressure ratio becomes lower, the diaphragm ruptures slower. If the extension tube becomes longer (α decreases), the time ratio of diaphragm rupture to pressure wave propagation in the tube becomes smaller. Therefore, in a high initial pressure ratio or in a low fill fraction, the experiments have good agreement with the simulations. Additionally, in the simulations, the model neglects friction and heat transfer and assumes constant specific heats.

Effect of initial pressure

The effect of the initial pressure ratio on the I_{sp} at a fixed fill fraction, $\alpha = 0.89$, is examined in Figure 12. The general trend is that the I_{sp} is larger at higher initial pressure ratios. A constant energy efficiency, $\eta = 0.30$, was used for the Gurney model solution. It shows close agreement with simulation results when $P_0/P_a > 4$, but overpredicts at lower pressure ratios due to the decrease in the energy efficiency at smaller pressure ratio. The simulation results are systematically higher than the experimental data. For helium, the computation results are larger than the experimental measurements by a factor of $1.5 - 1.7$

when $2.0 < P_0/P_a < 8.0$. For nitrogen, the discrepancy is large at small pressure ratio, i.e. a factor of ≈ 2.0 at $P_0/P_a = 2.0$, but smaller at high pressure ratio, i.e. a factor of ≈ 1.2 at $P_0/P_a = 9.38$. As shown in Fig. 11, the difference between experiments and simulations is large at $\alpha = 0.8$. We expect the agreement will be better at low fill fractions.

Model comparison

The ratios of $I_{sp}/I_{sp}(\alpha = 1)$ computed from the Gurney model, the Sato's model, and simulation results are shown in Fig. 13. Both models reasonably predict the I_{sp} when $0.2 < \alpha < 1.0$ at three pressure ratios. The Gurney model prediction is larger than the Sato's model prediction at all fill fractions and initial pressure ratios. The simulation results are smaller than both model predictions. Simulation results also show that the maximum ratio of $I_{sp}/I_{sp}(\alpha = 1)$ at $\alpha < 0.2$ is larger for lower pressure ratios, i.e. $I_{sp}/I_{sp}(\alpha = 1) \approx 2.7$ for $P_0/P_a = 3$, ≈ 1.8 for $P_0/P_a = 6$, and ≈ 1.5 for $P_0/P_a = 9.38$.

Energy efficiency

The ideal energy computed in section represents the maximum stored chemical energy in the pressurized gas. In reality, an energy efficiency η must be considered to represent the fraction of the stored chemical energy converted into mechanical work.[5] computed energy efficiency values based on predicted specific impulse values for several mixtures at initial conditions of 100 kPa and 300 K. Their work shows that efficiency values range between 0.124 and 0.305 for gaseous fuel-oxygen-nitrogen mixtures, which are slightly less than typical propellant efficiency values of $0.2 - 0.3$ and significantly less than typical efficiency values of $0.6 - 0.7$ for high explosives.

In the current study, the energy efficiency was computed by matching the Gurney model solutions with either the experimental measurements or simulations with least-square-fit criteria. Table 4 and Fig. 14 show the change in η at different pressure ratios for both helium and nitrogen. η is smaller at lower pressure ratios and larger for computations than experiments at all pressure ratios.

Conclusions

We used a shock tube with an open end to study the analog of the partial-fill effect observed in detonation tubes. We have carried out experiments and two-dimensional numerical simulations with a range of shock tube parameters. The specific impulse was measured and computed for two gases, helium and nitrogen, in the driver section and air in the driven section. The initial pressure ratio ranged from $P_0/P_a = 2.0$-9.38, and the fill fraction was varied from $\alpha = 0.05$-1.0. For both helium and nitrogen drivers, increasing the pressure ratio with a fixed fill fraction caused the specific impulse to increase. When the fill fraction

decreased, for helium, the specific impulse increased, and reached a maximum value when $\alpha < 0.2$, but the effect for nitrogen was negligibly small.

We also compared specific impulse results from numerical simulations, experimental measurements, and analytical models. The numerical simulation results matched reasonably well with experimental measurements for high pressure ratios ($P_0/P_a > 6$) over a large range of fill fractions ($\alpha = 0.05-0.8$), but a systematic difference existed when $\alpha > 0.8$ for all pressure ratios. We believe that these differences are associated with diaphragm opening time and curvature in the experiments, and neglecting heat transfer and friction in the simulations.

When the fill fraction is small ($\alpha < 0.2$), the analytical "bubble" model predicts a maximum specific impulse. The estimated value showed good agreement with both numerical computations and experiments for helium at three pressure ratios, 3.0, 6.0 and 9.38. The bubble model slightly under-predicted the impulse for nitrogen at high pressure ratios. When the fill fraction was sufficiently ($\alpha > 0.2$), the Gurney model predicts the correct trends but the effective energy is much lower than the ideal value and varies with the pressure ratios. Therefore, energy efficiencies must be determined empirically. The computed efficiencies range between 5% and 25% depending on the driver gas and fill fraction. By matching the specific impulse computed from the Gurney model with experimental data, we found the energy efficiency is much lower at smaller pressure ratios ($P_0/P_a = 3$: $\eta = 5.6\%$ for helium, $\eta = 7.3\%$ for nitrogen) than at larger pressure ratios ($P_0/P_a = 9.38$: $\eta = 17.8\%$ for helium, $\eta = 24.5\%$ for nitrogen). The Sato model and Gurney model yield very similar results and comparable level of agreement with the experiments or numerical simulations.

The dramatic differences between using nitrogen and helium for the driver shows that the partial-fill effect (increase in specific impulse with decreasing fill fraction) is primarily associated with wave processes and is not just due to inertia alone. The differences in density and sound speed between helium and air results in a sharp acoustic impedance discontinuity at the contract surface between the driver and driven section, this traps acoustic waves within the driver and results in the large increase in specific impulse observed in the helium cases. No such trapping occurs in the case of nitrogen and for this reason, the partial fill effect is not observed in this case. The acoustic analysis of the "bubble model" captures the difference between helium and nitrogen quantitatively at small fill fractions despite the nonlinear nature of the actual experiments. As the fill fraction approaches one and results in the decrease in specific impulse with increasing fill fraction. This is in agreement with the Gurney model for helium but not for nitrogen drivers. The disagreement of the Gurney, Sato, and other empirical models with the nitrogen cases indicates that energy conservation methods and mass ratios are insufficient to explain the partial-fill effect although these models show the correct trends for helium case. As the results for nitrogen show, the apparent agreement

is fortuitous and gas dynamic effects associated with the difference in sound speed between driver and driven section must be included in order to explain the partial-fill effect.

Acknowledgements

We thank R. Deiterding of DOE ASC Alliance Center for assistance in using the AMROC software, and also D. Lieberman, S. Jackson, and F. Pintgen for help with the experimental setup. We also thank Katsumi Tanaka, National Institute of Advanced Science and Technology, Japan, for his advice regarding the simulations and Hans Hornung, Caltech, for creating Fig. 2.

References

[1]Roy, G. D., Frolov, S. M., Borisov, A. A., and Netzer, D. W., "Pulse detonation propulsion: challenges, current status, and future perspective," *Prog. Energy Combust. Sci.*, Vol. 30, 2004, pp. 545–672.

[2]Zhdan, S. A., Mitrofanov, V. V., and Sychev, A. I., "Reactive Impulse from the Explosion of a Gas Mixture in a Semi-infinite Space," *Combustion, Explosion and Shock Waves*, Vol. 30, No. 5, 1994, pp. 657–663.

[3]Zitoun, R. and Desbordes, D., "Propulsive Performances of Pulsed Detonations," *Comb. Sci. Tech.*, Vol. 144, No. 1, 1999, pp. 93–114.

[4]Falempin, F., Bouchaud, D., Forrat, B., Desbordes, D., and Daniau, E., "Pulsed Detonation Engine Possible Application to Low Cost Tactical Missile and to Space Launcher," 37th AIAA/ASME/SAE/ASEE Joint Propulsion Conference and Exhibit, July 8–11, 2001, Salt Lake City, UT, AIAA 2001–3815.

[5]Cooper, M. and Shepherd, J. E., "The Effect of Nozzles and Extensions on Detonation Tube Performance," *AIAA 02-3628*, 2002.

[6]Cooper, M. A., *Impulse Generation by Detonation Tubes*, Ph.D. thesis, California Institute of Technology, Pasadena, California, May 2004.

[7]Cooper, M., Shepherd, J. E., and Schauer, F., "Impulse correlation for partially-filled tubes," *Journal of Propulsion and Power*, Vol. 20, No. 5, 2004, pp. 947–950, (Preprint - see journal for final version).

[8]Li, C. and Kailasanath, K., "Performance Analysis of Pulse Detonation Engines with Partial Fuel Filling," *Journal of Propulsion and Power*, Vol. 19 (5), 2003, pp. 908916.

[9]Kasahara, J., Arai, T., and Matsuo, A., "Experimental Analysis of Pulse Detonation Engine Performance by Pressure and Momentum Measurements," AIAA 03-0893.

[10]Kasahara, J., Tanahashi, Y., Hirano, M., Numata, T., Matsuo, A., and Endo, T., "Experimental Investigation of Momentum and Heat Transfer in Pulse Detonation Engine," AIAA 04-0869.

[11]Sato, S., Matsuo, A., Endo, T., and Kasahara, J., "Numerical Studies on Specific Impulse of Partially Filled Pulse Detonation Rocket Engines," *Journal of Propulsion and Power*, Vol. 22 (1), 2006, pp. 64–49.

[12]Kasahara, J., Tanahashi, Y., Numata, T., Matsuo, A., and Endo, T., "Experimental Studies on L/D Ratio and Heat Transfer in Pulse Detonations," 19th International Colloquium on the Dynamics of Explosion and Reactive Systems, Paper 65, July-August, 2003.

[13]Radulescu, M. I. and Hanson, R. K., "Effect of Heat Loss on Pulse-Detonation-Engine Flow Fields and Performance," *Journal of Propulsion and Power*, Vol. 21 (2), 2005.

[14]Wintenberger, E., Austin, J., Cooper, M., Jackson, S., and Shepherd, J. E., "An Analytical Model for the Impulse of a Single-Cycle Pulse Detonation Engine," *Journal of Propulsion and Power*, Vol. 19, No. 1, 2003, pp. 22–38.

[15]Cooper, M., Jackson, S., Austin, J., Wintenberger, E., and Shepherd, J. E., "Direct Experimental Impulse Measurements for Detonations and Deflagrations," *Journal of Propulsion and Power*, Vol. 18, No. 5, 2002, pp. 1033–1041.

[16]Deiterding, R., "High-resolution simulation of detonations with detailed chemistry," *In G. Warnecke, editor, Analysis and Numerics for Conservation Laws, pages 69-91, Springer, Berlin*, 2005.

[17]Deiterding, R., "A high-resolution method for realistic detonation structure simulation," *Proc. Tenth International Conference on Hyperbolic Problems: Theory, Numerics, Applications*, 2004.

[18]Gurney, R. W., "The initial velocites of fragments from bombs, shells, and grenades," Tech. rep., Army Ballistic Research Laboratory, 1943, Report BRL 405.

[19]Kennedy, J. E., "The Gurney Model of Explosive Output for Driving Metal," *Explosive Effects and Applications*, edited by J. A. Zuker and W. P. Walters, chap. 7, Springer, New York, 1998, pp. 221–257.

List of Tables

Table 1: Gas parameters.

Gas	γ	W (g/mol)	ρ @ 1atm (kg/m^3)
He	1.66	4.0	0.1787
N_2	1.406	28.0	1.2506
Air	1.4	29.0	1.225

Table 2: Specific impulse $I_{sp}(\alpha = 1)$ computed from the Gurney model, assuming an energy efficiency $\eta = 30\%$.

Gas	P_0/P_a	e_i (MJ/kg)	$I_{sp}(\alpha = 1)$ (s)
He	3.0	0.509	48.83
	6.0	0.965	67.25
	9.38	1.333	79.04
N_2	3.0	0.081	19.42
	6.0	0.146	26.17
	9.38	0.196	30.30

Table 3: Specific impulse $I_{sp}(\alpha \to 0)$ computed with the bubble model.

Gas	P_0/P_a	$I_{sp}(\alpha \to 0)$ (s)
He	3.0	105.04
	6.0	124.97
	9.38	128.57
N_2	3.0	18.79
	6.0	23.26
	9.38	24.61

Table 4: Energy efficiency η.

Gas	P_0/P_a	simulations	experiments
He	3.0	0.161	0.056
	6.0	0.197	0.153
	9.38	0.222	0.178
N_2	3.0	0.168	0.073
	6.0	0.229	0.229
	9.38	0.256	0.245

List of Figures

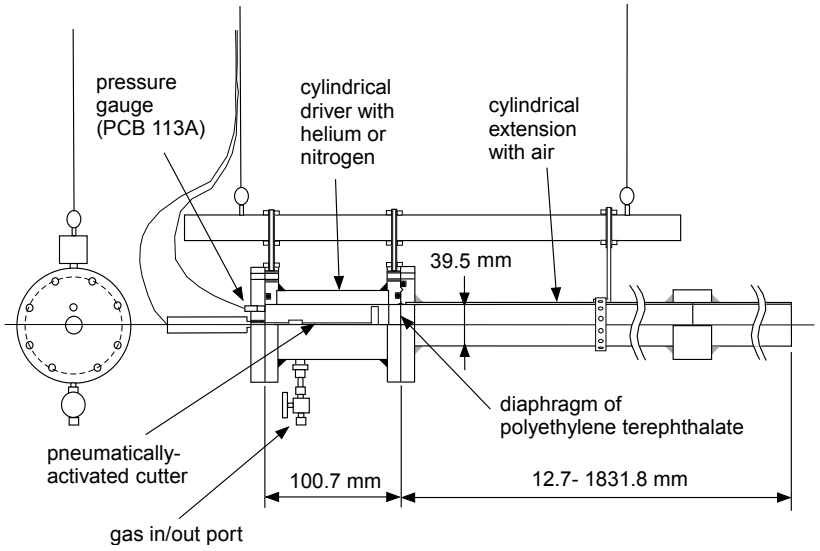

Figure 1: Partially-filled shock tube consisting of a cylindrical driver and cylindrical extensions.

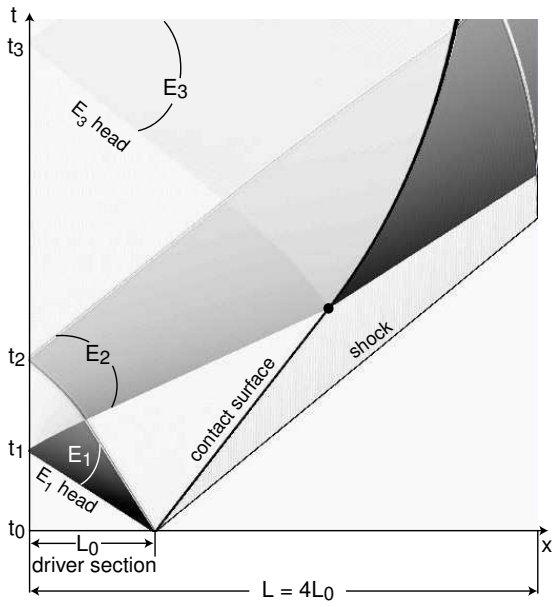

Figure 2: x-t diagram of inert gas dynamics in a partially-filled shock tube. E_1, E_2, **and** E_3 **represent the three expansion fans discussed in Section .**

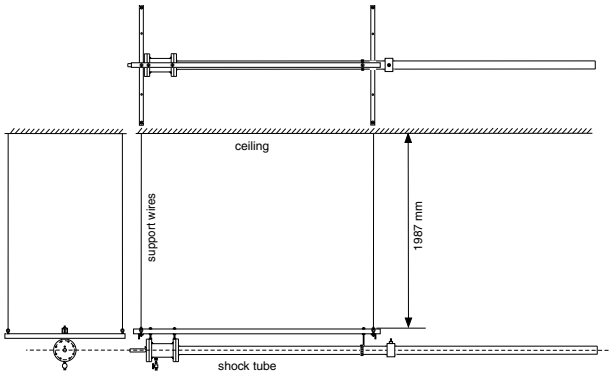

Figure 3: Experimental setup of the partially-filled shock tube.

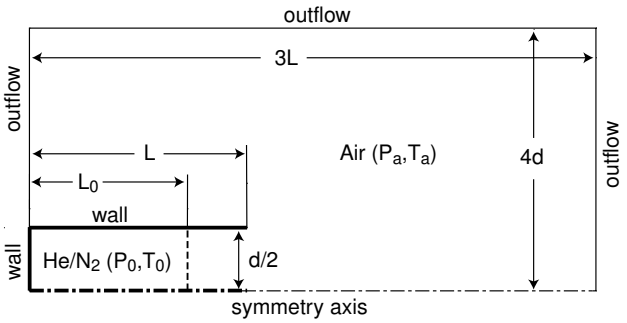

Figure 4: Computational model. L_0 = 101.6 mm, L = 0-1.84 m, d = 39.5 mm, P_a = 99 kPa, T_a = 295 K, P_0 = 198-929 kPa, T_0 =295 K.

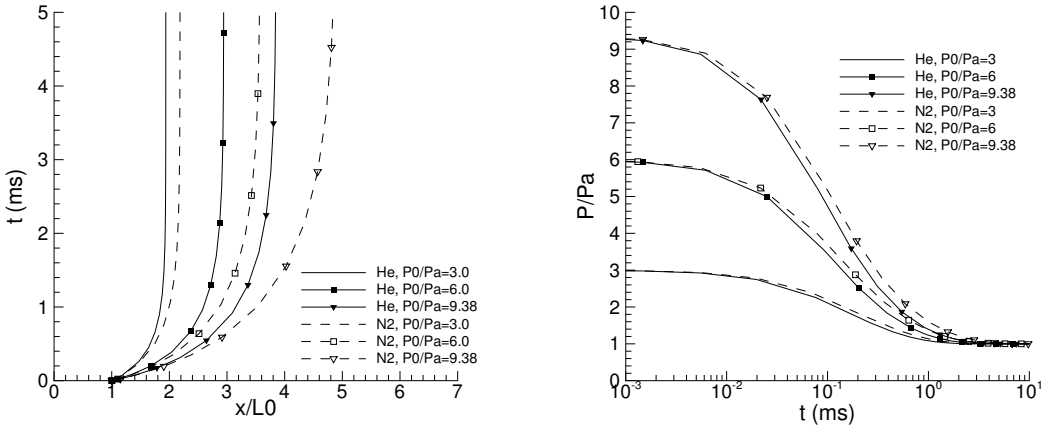

(a) (b)

Figure 5: (a) x-t diagram illustrating contact surface trajectory (b) Pressure histories illustrating pressure decay as a function of initial pressure ratio for the two isentropic exponents corresponding to each gas.

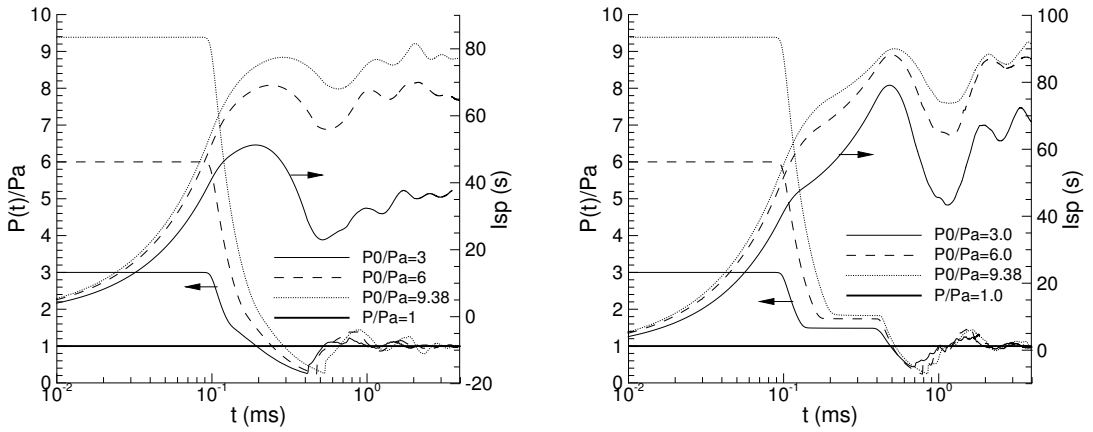

(a) (b)

Figure 6: Normalized pressure and specific impulse vs. time for (a) $\alpha = 1.0$ and (b) $\alpha = 0.6$ in He/Air.

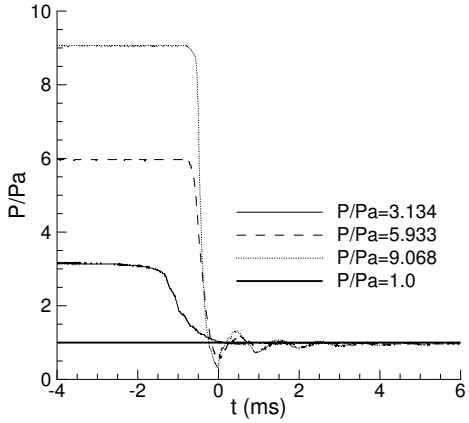

Figure 7: Experimental pressure profile at the thrust wall vs. time for $\alpha = 0.888$ in He/Air.

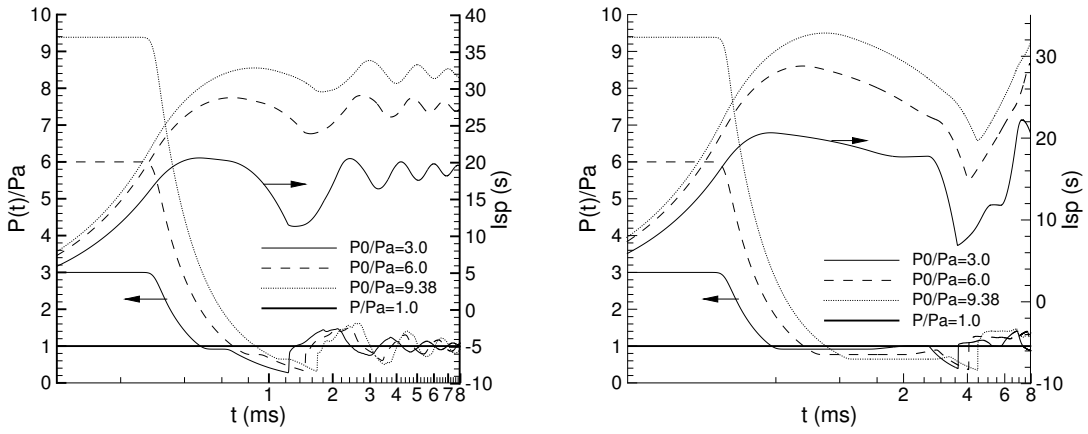

Figure 8: Normalized pressure and specific impulse vs. time for (a) $\alpha = 0.8$ and (b) $\alpha = 0.2$ in N_2/Air.

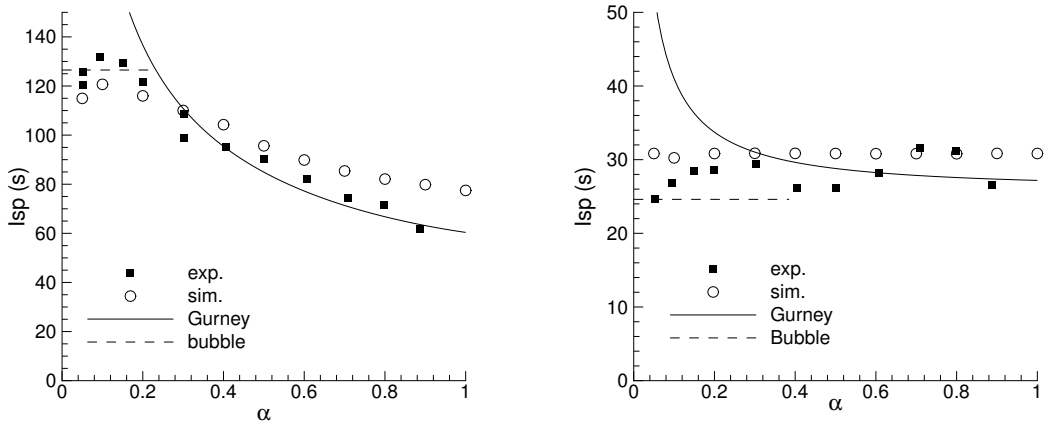

(a) (b)

Figure 9: Specific impulse vs. α for (a) He/Air and (b) N_2/Air. $P_0/P_a = 9.38$ for both simulations (sim.) and experiments (exp.). Gurney model energy efficiencies were: $\eta = 0.178$ for He/Air and $\eta = 0.245$ for N_2/Air.

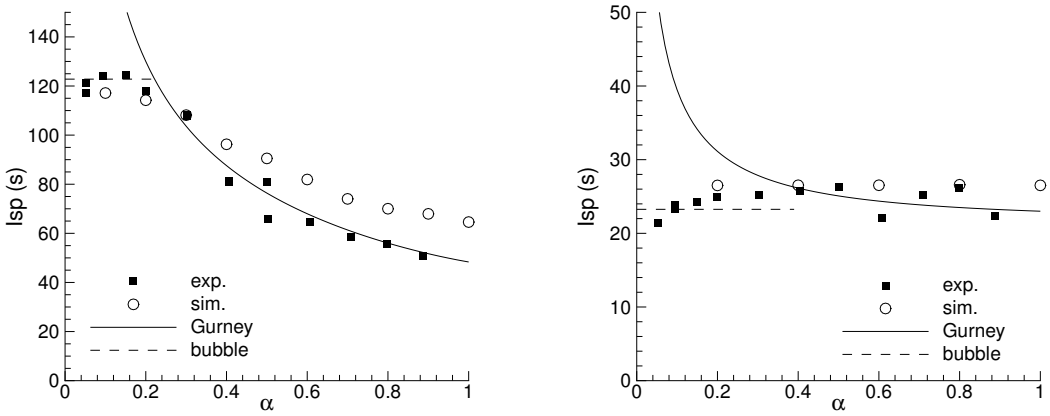

Figure 10: Specific impulse vs. α for (a) He/Air and (b) N_2/Air. $P_0/P_a = 6.0$ for simulations (sim.) and $P_0/P_a = 6.2$ for experiments (exp.). Gurney model energy efficiencies were: $\eta = 0.153$ for He/Air and $\eta = 0.229$ for N_2/Air.

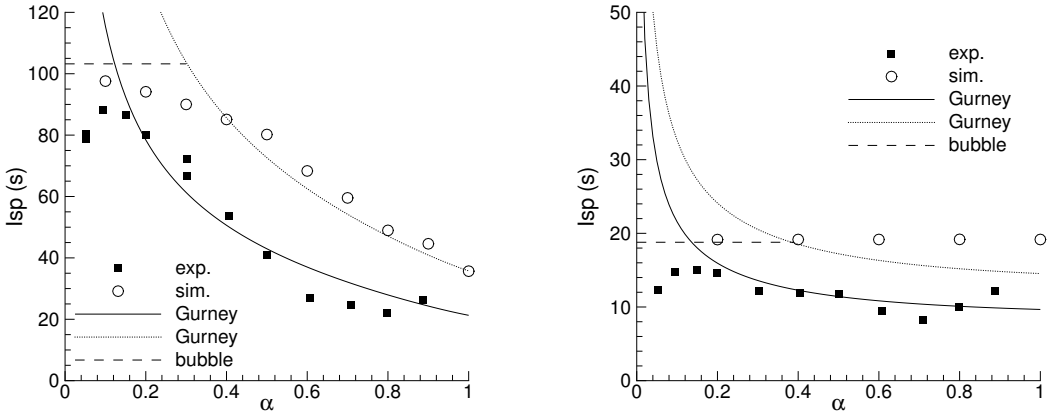

Figure 11: Specific impulse vs. α for (a) He/Air and (b) N_2/Air. $P_0/P_a = 3.0$ for simulations (sim.) and $P_0/P_a = 3.1$ for experiments (exp.). Gurney model energy efficiencies were: $\eta = 0.056$ (blue) and $\eta = 0.161$ (pink) for He/Air and $\eta = 0.073$ (blue) and $\eta = 0.168$ (pink) for N_2/Air.

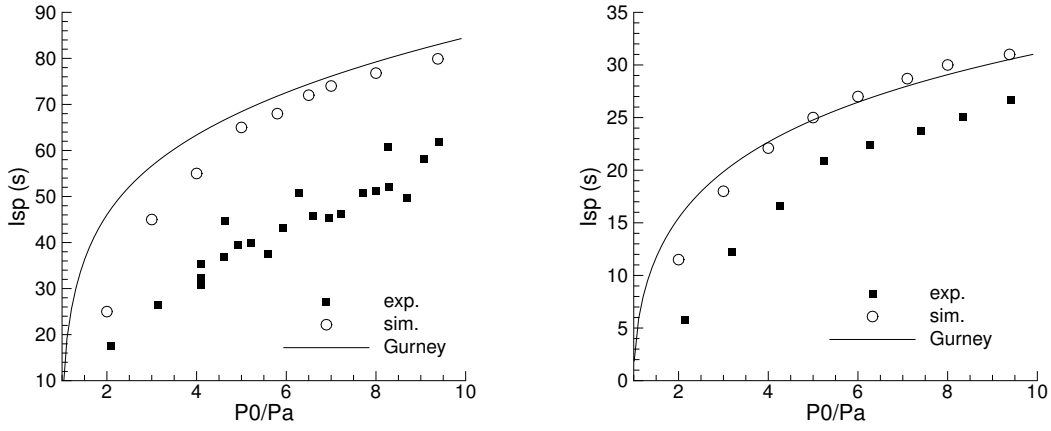

Figure 12: Specific impulse vs. pressure ratio for $\alpha = 0.89$ and (a) He/Air and (b) N_2/Air. The Gurney model energy efficiency was $\eta = 30\%$.

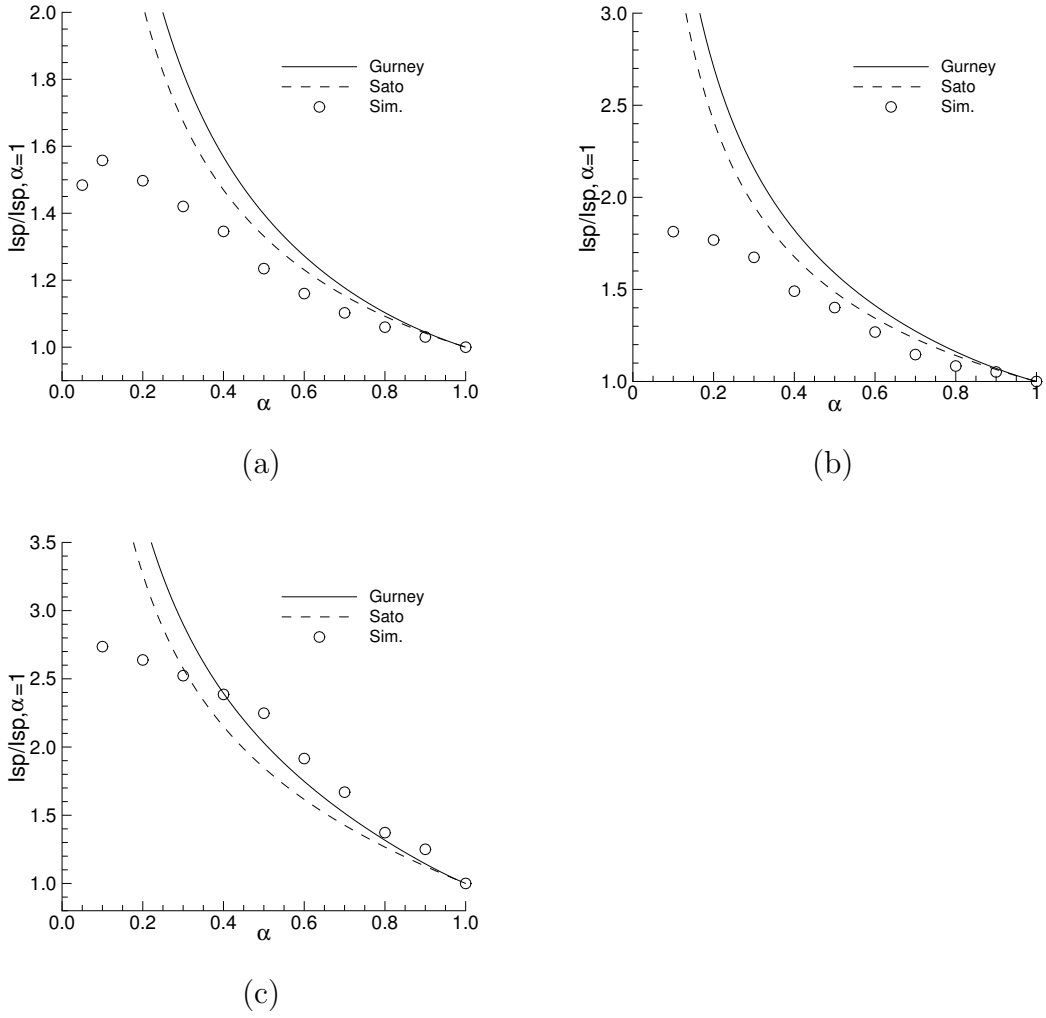

Figure 13: Specific impulse vs. fill fraction of He/Air for (a) $P_0/P_a = 9.38$, (b) $P_0/P_a = 6$ and (c) $P_0/P_a = 3$.

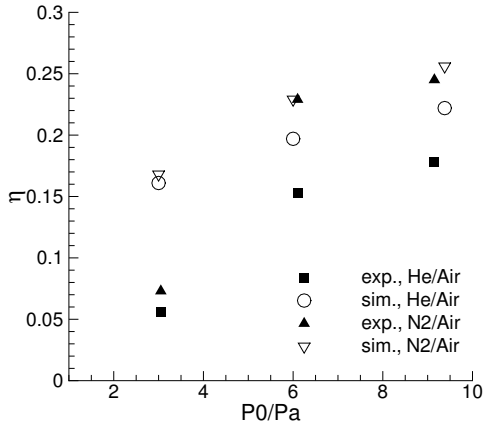

Figure 14: Energy efficiency η vs. pressure ratio P_0/P_a for both simulations and experiments, and He/Air and N_2/Air.